Journal of Molecular Structure 1265 (2022) 133414

Contents lists available at ScienceDirect

Journal of Molecular Structure

journal homepage: www.elsevier.com/locate/molstr

Synthesis, *in silico* and investigation of anti-breast cancer activity of new diphenyl urea derivatives: Experimental and computational study

Muhammed Gömeç[a], Koray Sayin[b,*], Mustafa Özkaraca[c], Hüseyin Özden[a]

[a] Department of General Surgery, Faculty of Medicine, Cumhuriyet University, Sivas, TÜRKİYE
[b] Department of Chemistry, Faculty of Science, Sivas Cumhuriyet University, Sivas, TÜRKİYE
[c] Department of Pathogy, Faculty of Veterinary, Cumhuriyet University, Sivas, TÜRKİYE

ARTICLE INFO

Article history:
Received 2 February 2022
Revised 29 May 2022
Accepted 30 May 2022
Available online 3 June 2022

Keywords:
Anticancer
Breast cancer
Diphenyl urea
In silico
In vitro
Synthesis

ABSTRACT

Cancer is a complex disease that requires multidisciplinary treatment. One of the most common cancers is breast cancer, and these cancers are usually estrogen receptor-positive. Today, chemotherapy, as well as surgery, has an important place in the treatment of cancer. For this reason, serious research is carried out on the search for new chemotherapeutic drugs. Some of the drugs currently used in breast cancer are targeted at the estrogen receptor. As a result of the preliminary analyses carried out within our study's scope, five new diphenylurea derivative compounds that we predict will be targeted to the estrogen receptor were determined and synthesized. Chemical analyzes of the synthesized compounds were performed. In addition, *in vitro* analyzes were performed for their biological effects. In this context, it was determined that DPU2, one of the compounds applied to the estrogen receptor (+) breast cancer cell line, MCF-7, showed the cytotoxic effect. The IC_{50} value was determined, and it was determined that although it showed a cytotoxic effect on MCF-7 cells, it did not show severe cytotoxicity in healthy fibroblast cells. Then, LC3B, one of the autophagy indicators, and IL-1β, a proinflammatory cytokine, were examined immunohistochemically. Both LC3B and IL-1β expression were lower in the DPU2 applied group than in the control group. These findings supported that DPU2 has antitumor activity on MCF-7. In conclusion, in the light of *in silico* and *in vitro* analyses conducted within the scope of our study, it was determined that DPU2, one of the five phenyl urea derivative compounds I synthesized, has the potential to be a drug in the treatment of estrogen receptor (+) breast cancer. However, the study needs to be supported by *in vivo* and clinical studies.

1. Introduction

According to the World Health Organization data, cancer is the cause of approximately 10 million deaths in 2020. Cancer, which is shown to cause one out of every six deaths, is the second most common cause of death. The most common types of cancer are breast, lung, and colorectal cancers. For this reason, the need for serious developments in breast cancer treatment continues today [1,2]. Many biological features affect the prognosis, response to treatment, and progression of this common malignancy. The most notable of these features is the estrogen receptor [3]. When subtypes of breast cancer are classified, they are classified according to whether they are hormone-dependent (ER(+) or ER(-)), and approximately 70% of breast cancer patients are ER(+) [4]. Therefore, ER has an essential role in treating breast cancer [5]. The ER, which plays a role in developing the female reproductive system, is divided into estrogen receptor beta (ER-β) and estrogen receptor alpha (ER-α). ER-β is found in the prostate gland, ovary, bladder, colon, immune system, and adipose tissue. ER-α is found in the mammary gland, ovary, uterus, testis, prostate, bone, liver, and adipose tissue [6]. It has also been reported that ER-α causes bladder and prostate cancer [7]. ER-α is thought to be effective in breast cancer by two possible mechanisms. The first of these hypotheses is that estrogen binds to the ER and triggers an excessive increase in cells, increasing harmful mutations resulting from insufficiency in DNA repair mechanisms [8]. Another hypothesis is that estrogen metabolism causes toxins that can directly cause DNA damage [9]. In addition, changes in ER-β in postmenopausal women have been shown to be effective in breast cancer [10]. Therefore, it can be said that both ERs may be influential in the development of breast cancer. Surgical resection alone may not be sufficient in the treatment of breast cancer. At this stage, chemotherapeutic agents come to the fore. New synthesis compounds come to the fore in the search for the most suitable chemotherapeutic agent. There-

* Corresponding author.
E-mail address: krysayin@gmail.com (K. Sayin).

https://doi.org/10.1016/j.molstruc.2022.133414
0022-2860/

fore, our study focused on new synthesis compounds that may be ER targeted.

Autophagy is a mechanism that has a severe effect on cell hemostasis, required to remove unnecessary proteins and dysfunctional organelles from the cell. Disruption in autophagy leads to severe metabolic stress in cancer cells. In this way, a severe inflammatory process occurs due to cell necrosis and the spread of these necrotic materials to the surrounding tissue. This leads to instability in cell DNA and a more aggressive phenotype [11]. One of the indicators of autophagy, which is the expression pathway of increased dysfunctional proteins due to the rapid proliferation of cancer cells, is the microtubule-associated protein LC3 (light-chain 3) [12]. Three types of LC3 have been reported in mammalian cells (LC3A, LC3B, LC3C). Of these, LC3B has a vital role in autophagosome formation. Therefore, LC3B is considered a vital autophagy marker [13]. Furthermore, an indicator of the inflammatory process that occurs due to tumor cells is the proinflammatory cytokine IL-1β, which is upregulated in many cancer types [14]. For all these reasons, we examined the effects of the DPU2 compound on LC3B and IL-1β expressions of MCF-7 breast cancer cells.

This study designed five new diphenyl urea compounds by computational chemistry techniques. These compounds are optimized at B3LYP-D3/6–31G(d) level in the water phase. The polarizable continuum model (PCM) using the integral equation formalism variant (IEF-PCM) model considers solute-solvent interactions. The electronic properties of this molecule are examined using contour plot of frontier molecular orbital, molecular electrostatic potential (MEP) map. Molecular docking calculations are performed against the estrogen receptor, which protein ID is 6VPK. Also, MM/GBSA analyses are performed for studied compounds. *In vitro* analyses of them are done against breast cancer cells for the first time. Finally, cytotoxic effects are examined via immunohistochemical techniques.

2. Materials and methods

2.1. Reagents

4′-Aminoacetophenone, 4-(trifluoromethyl)phenyl isocyanate, 3,5-bis(trifluoromethyl)phenyl isocyanate, 4–chloro-3-(trifluoromethyl)phenyl isocyanate, 3–chloro-4-methylphenyl isocyanate, 1-naphthyl isocyanate, and solvents which are toluene, DMSO was purchased from Merck kGaA.

2.2. Instrumentation

IR spectra (4000–400 cm^{-1}) were obtained using IR spectra (ATR) and recorded on a Bruker Tensor II FT-IR spectrometer. Melting points were measured on an Electrothermal IA9100 apparatus. ^{1}H-NMR and ^{13}C-NMR spectra were recorded on a JEOL (400 MHz) JNM-ECZ400S/L1 NMR instrument in DMSO–d_6 at room temperature; δ in ppm relative to tetramethylsilane (TMS), with J in hertz (Hz). Agilent Technology Inc. of 1260 Infinity HPLC System was coupled with 6530 Q-TOF LC/MS detector and ZORBAX SB-C18 (2.1 × 50 mm, 1.8 μm) column. ^{1}H NMR, ^{13}C NMR, and Q-TOF LC/MS analyses of the compounds were carried out at the Advanced Technology Application and Research Center (CUTAM) of Sivas Cumhuriyet University. Melting points were measured on an Electrothermal 9100 apparatus.

2.3. Synthesis of diphenyl urea (DPU) derivatives

To a solution of 4′-aminoacetophenone in toluene was added related isocyanate (1:1.2), and the mixture was refluxed for 3 h. The precipitate formed in the reaction was filtered and dried. Then, the obtained product was re-crystallized from DMSO [15]. The synthesized compounds are represented in Table 1. IR, ^{1}H NMR, ^{13}C NMR, and LC-QTOF-MS spectrum of synthesized compounds are given in Supp. Figs. S1–S20.

1-(4-acetylphenyl)−3-(4-(trifluoromethyl)phenyl)urea (**DPU1**). Brown solid. Yield 82%. Melting point: 226–229 °C. IR (KBr): 3332, 1683, 1668, 1599, 1587, 1541, 1514, 1415, 1400, 1362, 1320, 1270, 1243, 1209, 1178, 1159, 1110, 1064, 1010, 957, 839, 793 732, 632, 587, 567, 491. ^{1}H NMR (600 MHz, DMSO–d_6) δ 9.17 (s, 2H), 7.89 (d, J = 8.0 Hz, 2H), 7.66 (d, J = 7.9 Hz, 2H), 7.59 (dd, J = 15.4, 8.3 Hz, 4H), 2.48 (s, 1H). ^{13}C NMR (151 MHz, dmso) δ 196.72, 152.39, 144.35, 143.48, 131.19, 130.03 (2 C), 126.48 (q, J = 3.7 Hz), 124.92 (q, J = 271.0 Hz), 122.61 (q, J = 31.9 Hz), 118.53 (2C), 117.83 (2C), 26.70. HPLC-TOF/MS: 323.0851 ([M+H]$^+$, $C_{16}H_{13}F_3N_2O_2^+$; calc. 323.1002).

1-(4-acetylphenyl)−3-(3,5-bis(trifluoromethyl)phenyl)urea (**DPU2**). Brown solid. Yield 75%. Melting point: 228–231 °C. IR (KBr): 3372, 3302, 3203, 3116, 1725, 1646, 1601, 1572, 1539, 1473, 1390, 1333, 1279, 1167, 1122, 1039, 883, 833, 701, 676. ^{1}H NMR (600 MHz, dmso) δ 9.43 (s, 1H), 9.30 (s, 1H), 8.09 (s, 2H), 7.87 (d, J = 8.1 Hz, 2H), 7.65 – 7.48 (m, 3H), 2.47 (s, 3H). ^{13}C NMR (151 MHz, dmso) δ 196.70, 152.51, 144.06, 141.90, 131.16 (q, J = 32.7 Hz, 2C), 129.92 (2C), 123.67 (q, J = 272.7 Hz, 2C), 118.55, 118.13 (2C), 115.01, 26.66. HPLC-TOF/MS: 391.0709 ([M+H]$^+$, $C_{17}H_{12}F_6N_2O_2^+$; calc. 391.0876).

1-(4-Acetylphenyl)−3-[4–chloro-3-(trifluoromethyl)-phenyl]urea (**DPU3**). Brown solid. Yield 80%. Melting point: 257–260 °C. IR (KBr): 3330, 3258, 3157, 2950, 2886,1649, 1590, 1552, 1479, 1421, 1326, 1317, 1257, 1233,1178, 1128, 1035, 977, 831, 729, 629. ^{1}H NMR (600 MHz, DMSO) δ 9.23 (s, 1H), 9.22 (s, 1H), 8.08 (s, 1H), 7.89 (d, J = 7.6 Hz, 2H), 7.63 (d, J = 7.6 Hz, 1H), 7.58 (m, 3H), 2.49 (s, 3H). ^{13}C NMR (151 MHz, DMSO) δ 196.70, 152.51, 144.27, 139.40, 132.42, 131.24, 130.01 (2C), 127.19 (q, J = 30.6 Hz), 123.70, 123.21 (q, J = 272.9 Hz), 123.16, 117.95 (2C), 117.42 (q, J = 5.6 Hz), 26.74. HPLC-TOF/MS: 357.0667([M+H]$^+$,$C_{16}H_{13}ClF_3N_2O_2^+$; calc. 357.0612).

1-(4-Acetylphenyl)−3-(3–chloro-4-methylphenyl)-urea (**DPU4**). Brown solid. Yield 87%. Melting point: 222–225 °C. IR (KBr): 3369, 3288, 3193, 3107, 3061, 2976, 1717,1647, 1588, 1525, 1495, 1360, 1304, 1281, 1266, 1237,1189, 1167, 1045, 963, 912, 839, 828, 681, 596. ^{1}H NMR (600 MHz, DMSO) δ 9.09 (s, 1H), 8.85 (s, 1H), 7.88 (d, J = 7.2 Hz, 2H), 7.67 (s, 1H), 7.56 (d, J = 7.2 Hz, 2H), 7.30 – 7.10 (m, 2H), 2.49 (s, 3H), 2.24 (s, 3H). ^{13}C NMR (151 MHz, DMSO) δ 196.68, 152.51, 144.59, 138.91, 133.57, 131.61, 131.00, 130.04 (2C), 129.11, 118.83, 117.70 (2C), 117.64, 26.75, 19.25. HPLC-TOF/MS: 303.0820 ([M+H]$^+$,$C_{16}H_{16}ClN_2O_2^+$;calc. 303.0895).

1-(4-acetylphenyl)−3-(naphthalen-1-yl)urea (**DPU5**). Brown solid. Yield 82%. Melting point: 214–217 °C. IR (KBr): 3401, 3277, 3104, 3050, 1712, 1671, 1638, 1589, 1522, 1403, 1357, 1275, 1242, 1200, 1167, 973, 837, 783, 763, 660, 610. ^{1}H NMR (600 MHz, DMSO) δ 9.46 (s, 1H), 8.89 (s, 1H), 8.13 (d, J = 5.4 Hz, 1H), 8.04 (d, J = 3.5 Hz, 1H), 7.92 (bs, 3H), 7.66 (bs, 3H), 7.58 (s, 1H), 7.49 (m, 2H), 2.50 (s, 3H). ^{13}C NMR (151 MHz, DMSO) δ 196.71, 153.10, 144.87, 134.36, 134.17, 130.94, 130.16 (2C), 128.88, 126.61, 126.38, 126.27, 126.25, 123.88, 121.79, 118.41, 117.60 (2C), 26.71. HPLC-TOF/MS: 305,1161 ([M+H]$^+$, $C_{19}H_{16}N_2O_2^+$; calc. 305.1285).

2.4. Computational chemistry

Gaussian software was used in the computational investigations [16,17]. The mentioned compounds were optimized at the B3LYP-D3 method with 6–31G(d) basis set in water. Additionally, the polarizable Continuum Model (PCM) using the integral equation formalism variant (IEF-PCM) was considered solute-solvent interactions. At the results of calculations, no imaginary frequency was observed. IR and NMR spectrums were calculated at the same level

Table 1
Synthesized compounds and their assignments.

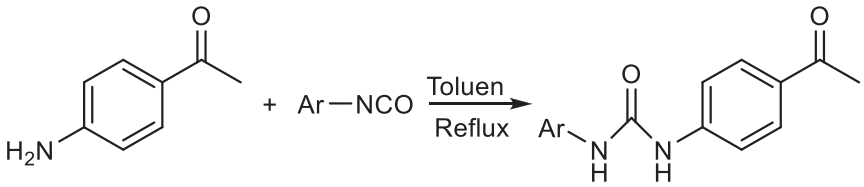

Assignment	Compound Structure
DPU1	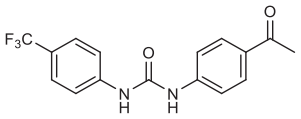
DPU2	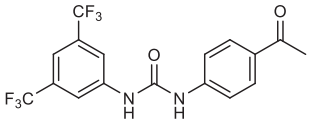
DPU3	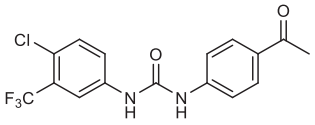
DPU4	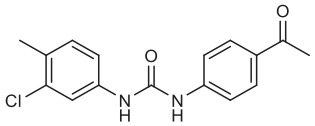
DPU5	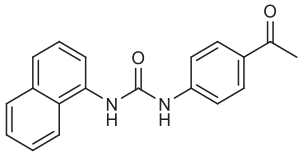

of theory. Some utilities, such as ChemDraw, were used in this study [18].

2.5. Molecular docking and adme

The ground state structures of phenyl urea derivatives were obtained from computational calculations. The Maestro program was used [19–22]. Furthermore, the Maestro program has been used in many investigations of ligand-protein interactions [23–28]. The ligand and target protein were prepared using LigPrep and Protein Preparation modules. The receptor-binding domain of the target protein was defined using the Grid Generation module. pH was defined as 7 ± 2 in the whole calculations. Molecular docking calculations were performed using the Ligand Docking module. Molecular mechanics energies combined with the generalized Born and surface area continuum solvation (MM/GBSA) calculations are performed at the Maestro program. Binding energy ($_{binding}$) was calculated using Eq. (1).

$$E_{Binding} = E_{Complex} - E_{Protein} - E_{Ligand} \quad (1)$$

where $_{complex}$, $E_{Protein}$, and E_{Ligand} Show the complex energy, only protein energy, and only ligand energy, respectively.

2.6. Cell culture studies and development of MCF-7

In this study, the human breast cancer cell line MCF7 obtained from the American Type Culture Collection (ATCC, Manassas, VA, USA) was used. Cells were cultured in 25cm^2 flasks containing RPMI containing 10% Fetal Bovine Serum (FBS), 1% penicillin/streptomycin, and 1% L-glutamine. Cells were maintained at 37 °C in a humidified atmosphere with 5% CO2. Cells reaching 80% density were passaged. Cells were seeded on a 96- plate so that the number of cells in each well was 1 × 10^4 cells. The new synthesis compounds were dissolved in DMSO and diluted in a culture medium before being treated with a final DMSO content of 5%.

2.7. Cell viability assay

Breast cancer cell line MCF-7 was used to evaluate the anticancer activity of our newly synthesized DPU1-DPU5 compounds. The TXT colorimetric method (2,3-bis-(2–methoxy-4-nitro-5-sulphophenyl)−5-[(phenylamino)carbonyl]−2H-tetrazolium hydroxide) (Biological Industries) was used to assess cell viability. MCF-7 cells in the growth phase were seeded at a density of 1 × 10^4 cells per well in 96-well microplates prepared in RPMI 1640 culture medium (100-µL). After 24 h of incubation, the process was started. Five synthesis compounds were administered separately at a dose of 20 µM to both cell lines. Cells were classified as the control group and drug group. No application was made to the control group. Five synthesis compounds (DPU1, DPU2, DPU3, DPU4, and DPU5) were administered separately at a dose of 20 µM to both cell lines. It was kept in the incubator for 24 h. After incubation, the 96-well plate was removed, and the wells were washed with phosphate-buffered saline (PBS). Then, 100 µL of phenol red-free DMEM and 50 µL of TXT solution were added to all wells, and then the plates were kept at 37 °C for 4 h. Absorbance values were determined at 450 nm using an ELISA microplate reader (Thermo Fisher Scientific, Altrincham, UK). This procedure was repeated three times. Cell viability was accepted as 100% in the control group. Cell viability was calculated using

the formula (% Cell viability = (Concentration O.D./Control O.D.) X 100). Of the five compounds, only DPU2 was observed to have a severe cytotoxic effect on MCF-7 cells. In order to determine the IC50 value of the DPU2 compound, which has a good cytotoxic effect on MCF-7 at 20 µM dose, the DPU2 compound was applied to MCF-7 at different doses (80, 40, 20, 10.5 µM). The IC_{50} value (drug concentration causing 50% reduction in proliferation) was calculated using Graph Prism 7 software (GraphPad). Next, the possible cytotoxic effect on the healthy connective tissue cell line L929 was investigated to investigate the selectivity of the DPU2 synthesis compound to tumor cells. Compound DPU2 was administered to the L929 cell line at the same doses (80, 40, 20, 10.5 µM). The cytotoxic effects of the new synthesis compound DPU2 on MCF-7 and L929 were compared.

2.8. Immunofluorescence examination

The prepared cells were fixed with methanol for 5 min at −20 ºC. It was then washed with PBS and incubated for 15 min at room temperature with PBS containing 0.1% Triton X-100. Then, PBS containing 2% BSA was prepared and incubated at room temperature for 60 min after washing. Washing was done again, then monoclonal anti-MAP LC3B (Santa Cruz, Catalog no. sc-271,625) and monoclonal anti-IL-1β (Santa Cruz, catalog no. sc-52,012) primary antibodies at a dilution rate of 1/300 at +4ºC' was incubated overnight. The cells prepared by washing with PBS were incubated with goat anti-mouse FITC secondary antibody at a dilution ratio of 1/50 for 1 h at room temperature in the dark, compatible with the primary antibodies used. After all these procedures, DAPI (4′,6-diamidino-2-phenylindole) was dropped on the washed cells and examined under a fluorescence microscope. All fields were taken into account while making the evaluation. The rate of positivity in cells was evaluated semiquantitatively as absent (-), mild (+), moderate (++), and severe (+++).

2.9. Statistical analyses

All the data obtained were analyzed with the SPSS 23.0 package program. Data obtained as a result of immunofluorescence analysis were analyzed with Student's T-test. Results of cell culture studies were expressed as mean ± standard deviation (SEM). Data were evaluated using a one-way analysis of variance (ANOVA). The post hoc Tukey test was used to determine the differences between the experimental groups. The significance level was accepted as $p<0.05$.

3. Results and discussion

3.1. Optimized structures

The synthesized compounds are optimized at B3LYP-D3/6–31G(d) level in the water using Gaussian software. Optimized structures are represented in Fig. 1 with atomic labeling.

According to Fig. 1, the compound structure is generally planar. Some geometric parameters of them are given in Supp. Table S1. According to this table, the geometric parameters are similar to each other. There are no significant differences.

3.2. Simulated IR spectra

IR spectrum of the related compounds is calculated at the same level of theory. Vibrational energy distribution analyses are done using the VEDA4XX program. The vibrational frequencies and their assignment are given in Supp. Table S2. Furthermore, the calculated spectrum of studied compounds is given in Supp. Figs. S21–S25 for DPU1 – DPU5, respectively. According to Supp. Table S2, the calculated frequencies are in good agreement with the literature and their experimental results [15]. However, some differences in frequency values are noteworthy. The main reason for this difference is that the experimental frequency is anharmonic, and the computational frequency is harmonic. In the IR spectrum analysis, The VEDA 4XX program is very effective in identifying vibration modes and tagging frequencies.

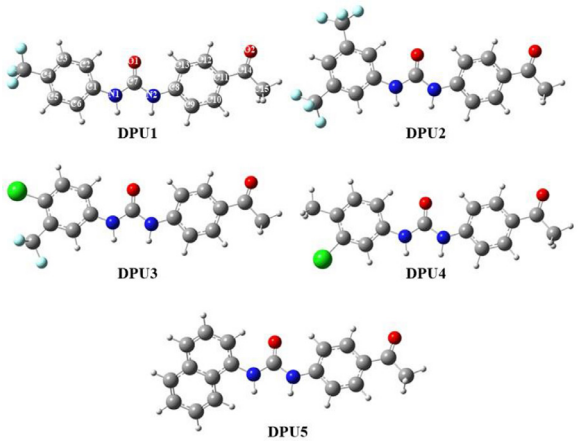

Fig. 1. The optimized structure of studied diphenyl ureas.

3.4. Electronic properties

Determination of electronic properties of compounds is essential for discovering chemical properties. Some pictures or figures, contour diagrams of frontier molecular orbitals, and molecular electrostatic potential (MEP) maps can be used. In this study, contour plots of HOMO/LUMO and MEP maps are used. Contour plots of frontier molecular orbitals are calculated and represented in Fig. 2.

According to Fig. 2, HOMO electrons are delocalized on the whole structure of the studied compound. Primarily, it is observed that π electrons play an essential role in having this feature. As for the contour plot of Lumos, electrons are mainly localized on the left side of the molecules. The benzaldehyde group in the studied compounds seems more reactive than the other side of the molecules.

MEP map can be used in determining the electronic properties of the compounds. While the contour plot of frontier molecular orbitals shows special zones that can be active, MEP maps show regions on the molecule's surface that can interact. MEP maps of the studied compounds are calculated and represented in Fig. 3.

According to Fig. 3, the surface of compounds is colorful. The observed colors have the meaning chemically. The red color implies the electron-rich region, while the dark blue indicates the electron-poor region. Generally, the environment of oxygen atoms in the carboxyl group is mainly red, and this region is appropriate for the electrophilic attack, while the dark blue region is appropriate for the nucleophilic attack.

3.5. Molecular docking and mm-gbsa analysis

Determination of the biological activity of compounds is significant, and it can be determined experimentally and computationally. In this study, estrogen receptor (ER) is selected as the target protein, and it is known that inhibition of estrogen receptor is one of the anti-cancer mechanisms. Also, ER is positive in approximately 60% of breast cancer patients. 6VPK is selected as the target protein in the docking calculations, and this protein chain

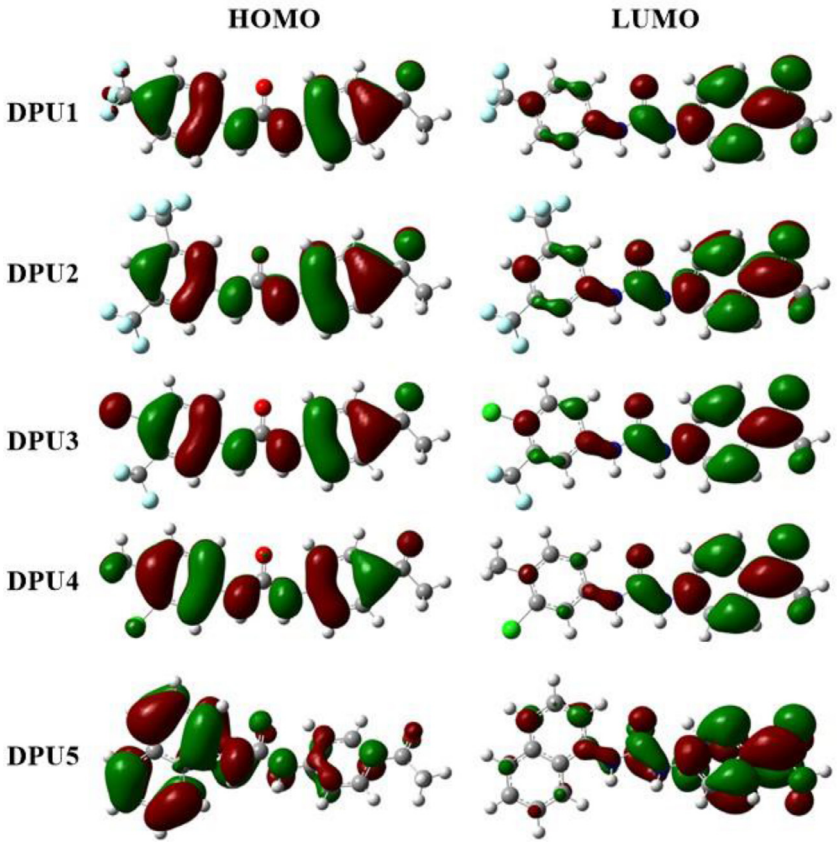

Fig. 2. Contour diagram of frontier molecular orbitals.

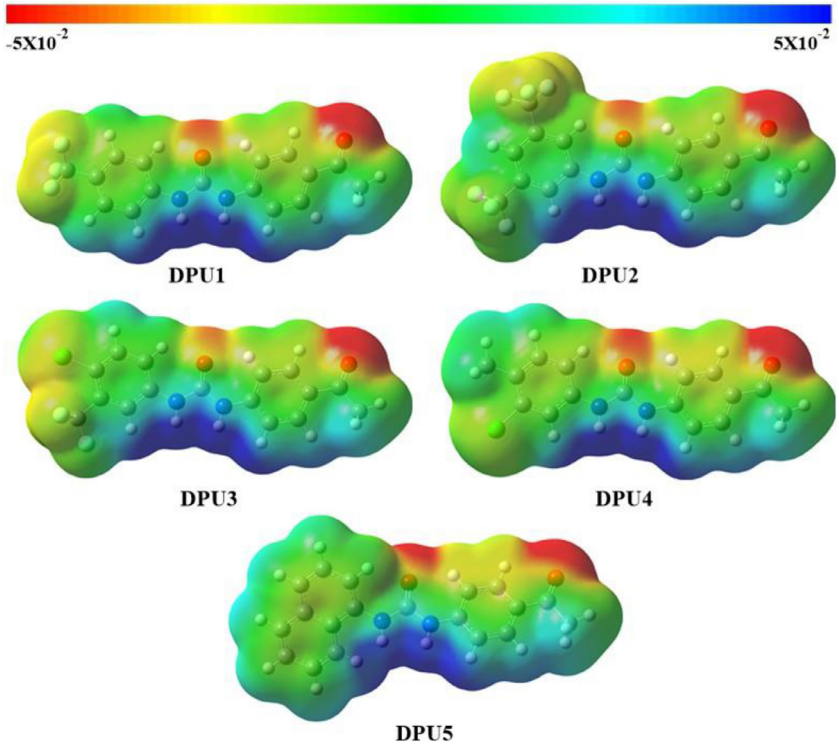

Fig. 3. MEP maps of the studied compounds.

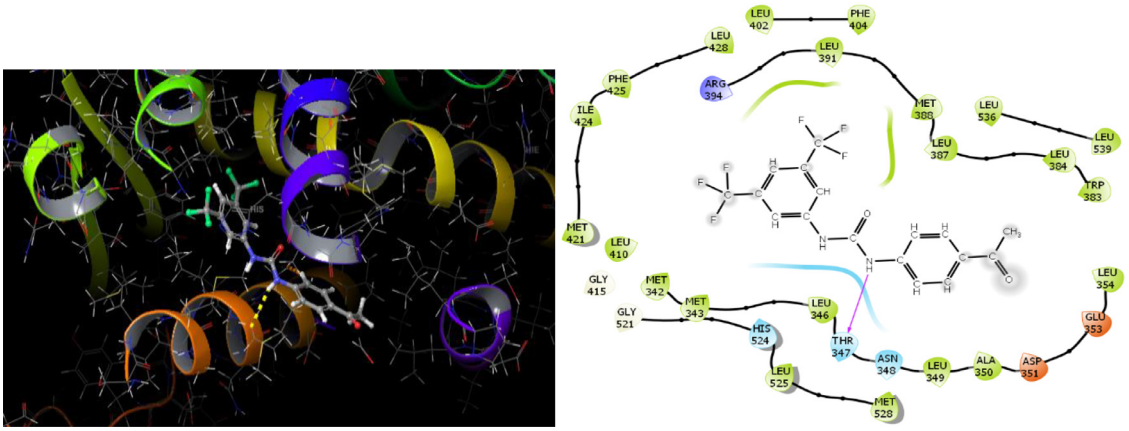

Fig. 4. The complex structure (left) and interaction structure (right) of DPU2.

Table 2
Molecular docking results between studied compounds and RBD of A chain of 6VPK.

Compound	DS[A]	E_{vdW}[a]	E_{Coul}[a]	E_{Total}[a]
DPU1	−6.369	−36.187	−1.107	−37.295
DPU2	−6.433	−36.871	−1.880	−38.751
DPU3	−5.593	−34.258	−1.864	−36.122
DPU4	−6.169	−41.096	−0.585	−41.682
DPU5	−6.178	−35.272	−2.127	−37.399

[a] in kcal/mol.

Table 3
The MM/GBSA results.

Compound	$E_{Complex}$[a]	$E_{Protein}$[a]	E_{Ligand}[a]	$E_{Binding}$[a]
DPU1	−9175.846	−9095.407	−36.501	−43.937
DPU2	−9180.992	−9095.407	−30.187	−55.398
DPU3	−9177.304	−9095.407	−43.352	−38.545
DPU4	−9190.079	−9095.407	−41.588	−53.084
DPU5	−9156.968	−9095.407	−20.509	−41.052

[a] in kcal/mol.

is considered in the analyses. Studied compounds are prepared for docking calculation at pH=7 ± 2 using the LigPrep module.

Furthermore, the selected protein is prepared at the OPLS3 method using the ProteinPreperation module. The SiteMap module determines its active regions. The active region and receptor bind domain of this protein is represented in Supp. Figs. S26–S29. Also, the x-y-z coordinates of these regions are given in Supp. Table S3. Molecular docking calculations are performed between the studied ligand and active regions in the selected protein. In this analysis, the ligand was considered flexible, while the target sites of the protein were considered partially flexible. The docking calculations are performed, and the docking score (DS), van der Walls interaction energy (E_{vdW}), Coloumb interaction energy (E_{Coul}), and total interaction energy (E_{Total}) for the receptor-binding domain (RBD) are given in Table 2. In this stage, other results are given in Supp. Tables S4–S6.

According to Table 2, the best docking score is observed in DPU2. The docking score is so important to determine the key-lock compatibility between inhibitor candidate and target protein. For this reason, the first parameter in determining the best compound is the docking score. As for the interaction energies, calculated total interaction energies are nearly similar. However, it can be said that DPU4 has the best value in this stage. As a result, the best candidate for the inhibition of the estrogen receptor is DPU2. The complex structure and interaction map of DPU2 are represented in Fig. 4.

Molecular docking calculations are performed for other active binding domains. It is observed that DPU1 is found to be the best inhibitor candidate. On the other hand, DPU2 is the worst compound for the active binding domain (ABD) except ABD3. It is observed that the affinity of DPU2 to the receptor-binding site is very high compared to other active binding domains, and therefore, the selectivity of DPU2 to RBD is high. Since this situation is critical in silencing the target receptor, it is predicted that DPU2 may also show effective results in experimental studies. In addition to molecular docking analyses, the molecular mechanics energies combined with the generalized Born and surface area continuum solvation (MM/GBSA) analysis are performed for only RBD of 6VPK. The binding energies for each complex structure are calculated using Eq. (1) and given in Table 3.

According to Table 3, the best binding energy is obtained in DPU2. The lower the binding energy, the stronger the interaction between the ligand and the protein. Therefore, it can be said that DPU2 can be a good candidate for inhibiting estrogen receptor.

3.6. Biological activity

Within the scope of the study, estrogen receptor (+) breast cancer cell line MCF-7 was used to evaluate the anti-cancer activities of newly synthesized diphenyl urea derivative compounds. In the first step, all compounds were administered to the MCF-7 cell line at a fixed concentration of 20 µM. Cell viability percentages were calculated by TXT colorimetric method 24 h after the application. Results below 55% were considered significant. The study was repeated three times. Cell viability values; DPU1=95%, DPU2=51%, DPU3=86.33%, DPU4=85.67%, DPU5=91.33%. As a result of the statistical analysis, it was determined that DPU2, DPU3, DPU4, and DPU5 compounds showed cytotoxic effects. However, DPU2 providing cell viability below 55% was selected for further studies (Table 4).

At this stage of the study, the IC50 value of the DPU2 compound that was effective in the MCF-7 cell line was determined. DPU2 compound was applied to the MCF-7 cell line at doses of 5 μM, 10 μM, 20 μM, 40 μM, 80 μM. Cell viability was obtained by TXT. Average cell viability rates are obtained from three replicates; It was 99.66% at 5 μM, 80% at 10 μM, 48% at 20 μM, 35% at 40 μM, and 29.67% at 80 μM. Therefore, the IC50 value was found to be 14.11 µM. In another phase of the study, the potential cytotoxicity of DPU2 was examined on the healthy fibroblast cell line L929 at the same doses (5 μM, 10 μM, 20 μM, 40 μM, 80 μM). The mean cell viability values were obtained by XTT performed at the end of three repetitions. The IC50 value was determined as 14.11 µM. In another phase of the study, the potential cytotoxicity of DPU2

Table 4
Results of administration of 20 µM of IS compounds in MCF-7 Cell Lines.

	MCF-7 (Brest Cancer)		
	n	***Mean±Std. Error***	***p***
Control	3	100	–
DPU1	3	95 ± 0.57	$p = 0.419$
DPU2	3	51 ± 1.15*	$p < 0.05$
DPU3	3	86.33 ± 3.53	$p < 0.05$
DPU4	3	85.67 ± 1.86	$p < 0.05$
DPU5	3	91.33 ± 1.45	$p < 0.05$

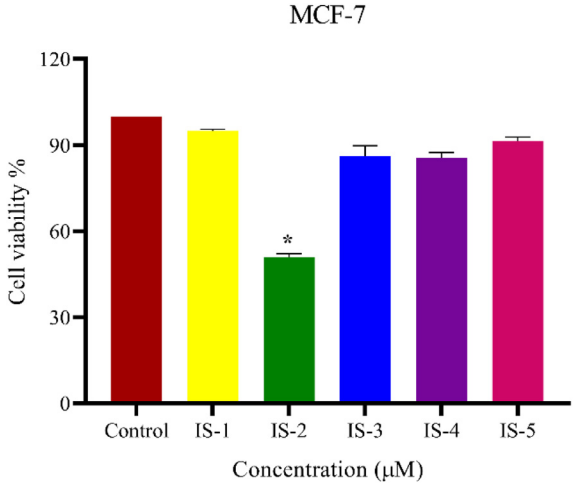

Table 5
The efficacy of DPU2 synthesis compound at doses of 5 μM, 10 μM, 20 μM, 40 μM, 80 μM in MCF-7 and L929 cell lines is shown in the table and graph.

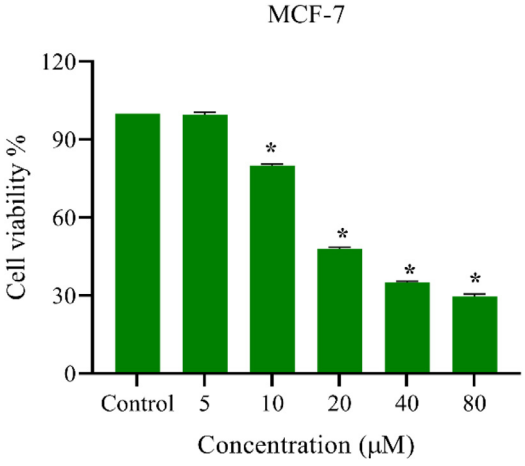

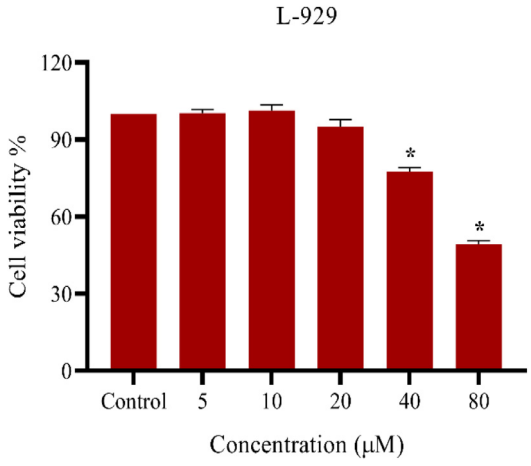

	MCF-7(Brest cancer)			*L-929 (Fibroblast)*		
DPU2 Dose	***n***	***Mean±Std. Error***	***P***	***n***	***Mean±Std. Error***	***P***
Control	3	100	–	3	100	–
5 µM	3	99.66±0.88	$p = 0.999$	3	100.33±1.45	$p = 1.000$
10 µM	3	80.00±0.58	$p < 0.05$	3	101.33±2.33	$p = 0.995$
20 µM	3	48.00±0.58	$p < 0.05$	3	95,00±2,89	$P = 0.430$
40 µM	3	35.00±0.58	$p < 0.05$	3	77,67±1,45	$p < 0.05$
80 µM	3	29.67±0.88	$p < 0.05$	3	49,33±1,45	$p < 0.05$

was examined on the healthy fibroblast cell line L929 at the same doses (5 μM, 10 μM, 20 μM, 40 μM, 80 μM) (Table 5).

In conclusion, although DPU2, a new diphenylurea derivative compound we synthesized, has a severe cytotoxic effect on the estrogen receptor (+) human breast cancer cell line MCF-7, It was determined that it did not show a significant cytotoxic effect on the healthy fibroblast cell line L929.

3.8. Immunofluorescence findings

The effect of DPU2, which was found to have a cytotoxic effect in the MCF-7 cell line, was demonstrated by staining with LC3B and IL-1β. Statistically significant differences were detected between the groups in the immunofluorescence examination (Fig. 5, p <0.05).

While LC3B expression was severe in the MCF-7 cell line control group, LC3B expression level was mild in the MCF-7 group treated with DPU2. While IL-1β was moderately expressed in the control group, no significant IL-1β expression was detected in the DPU2 administered group. The detected fluorescence positivity was intracytoplasmic localized (Figs. 6 and 7).

One of the most common biomarkers in various cancers is the immunohistochemical analysis of LC3B, one of the autophagy proteins in tumor cells [29,30]. Generally, it is known that LC3B expression is high in cancer cells. In a study they conducted, Zheng

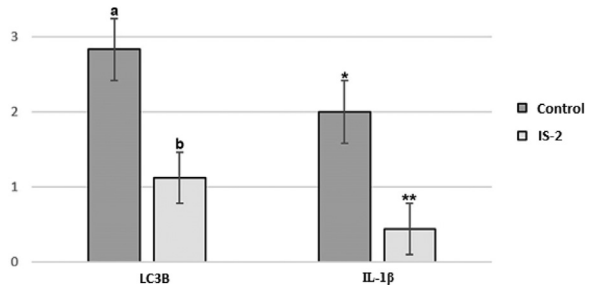

Fig. 5. Statistically LC3B and IL-1β expression levels. (a,b,*,** indicate the difference between groups, p <0.05).

et al. [31] attributed the aggression of colorectal cancer cells and their adaptation ability against apoptosis to autophagy. They examined LC3B as an indicator of autophagy. As in many cancer types, high LC3B expression in breast cancer has been reported to be an indicator of both a poor prognosis and an aggressive course [32]. Zhao et al. [33] reported that LC3B could be used as a marker in triple-negative breast cancer in a study they conducted. Our study observed that the DPU2 synthesis compound significantly decreased the LC3B expression of MCF-7 breast cancer cells compared to the control group.

IL-1β is an inflammatory cytokine. It is increased both in chronic inflammation and in the presence of tumors [34]. It is known that IL-1β may be influential in cancer cell proliferation, angiogenesis, cell migration, and metastasis [35]. Cui et al. reported in their study that there is a high level of IL-1β in the tumor microenvironment in human colorectal cancers, which is vital in the progression of the tumor [36]. There is a relationship between IL-1β exploration and survival in breast cancer. Increased expression of IL-1β has been shown to decrease survival in breast cancer [37]. Therefore, IL-1β expression was studied to evaluate the efficacy of DPU2, which shows its cytotoxic effect on MCF-7. It was observed that DPU2 significantly decreased the expression of IL-1β in MCF-7 cells.

Both the reduction of LC3B, which is one of the indicators of autophagy, and the decrease of IL-1β, which has a high expression potential in cancer cells, have shown us that the DPU2 compound may have anti-cancer severe activity in the breast cancer cell line MCF-7.

4. Conclusion

Within the scope of our study, diphenylurea derivative compounds were investigated, and five diphenylurea derivative compounds, which we predicted to be effective in Estrogen receptor (+) breast cancers, were determined by *in silico* analysis. We syn-

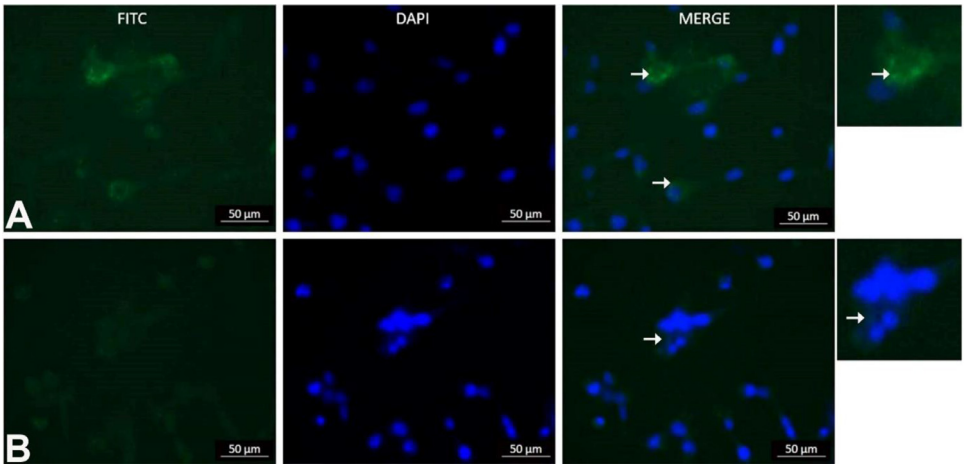

Fig. 6. A- Severe LC3B positivity in the control group, B- Mild LC3B positivity in the DPU2 group (arrows).

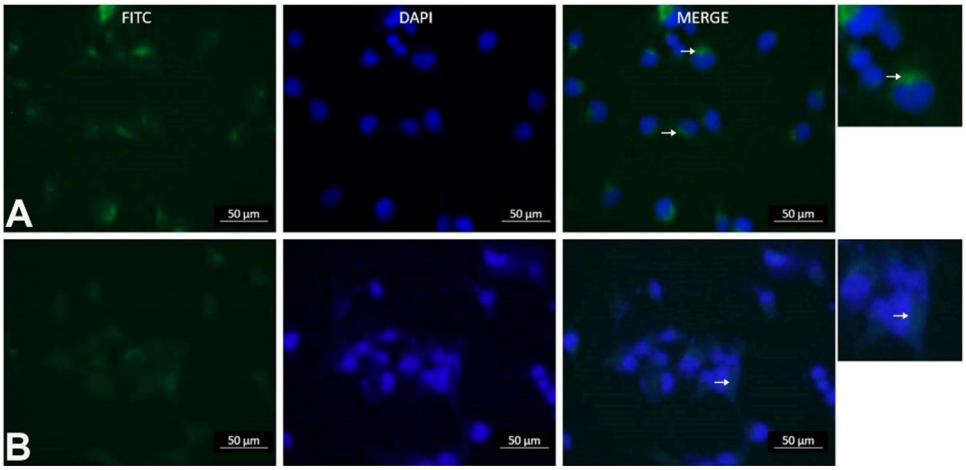

Fig. 7. A- Moderate IL-1β positivity in the control group, B- IL-1β negativity in the DPU2 group (arrows).

thesized these five original compounds and made their chemical analysis. We conducted *in vitro* studies to examine the biological activities of these compounds. In this context, the compounds were applied to the ER(+) breast cancer cell line MCF-7. Of these five compounds, DPU2 was found to have a severe cytotoxic effect on MCF-7. In addition, the compounds were administered to L929 healthy fibroblast cells at the same doses. According to the results obtained, it was determined that DPU2 did not show a cytotoxic effect in breast cancer cells in L929 cells. In addition, this effect was confirmed by immunohistochemical studies. In light of all these results, it has been shown that our newly synthesized DPU2 can contribute to breast cancer treatment. Our study should be supported by *in vivo* and clinical studies.

Declaration of Competing Interest

The authors declare that they have no known competing financial interests or personal relationships that could have appeared to influence the work reported in this paper.

CRediT authorship contribution statement

Muhammed Gömeç: Formal analysis, Writing – original draft, Writing – review & editing. **Koray Sayin:** Writing – original draft, Writing – review & editing, Methodology, Formal analysis. **Mustafa Özkaraca:** Writing – original draft. **Hüseyin Özden:** Writing – review & editing.

Acknowledgement

This work is supported by the Scientific Research Project Fund of Sivas Cumhuriyet University under the project numbers RGD-020, RGD-036 and T-2021–921. This research was made possible by TUBITAK ULAKBIM, High Performance, and Grid Computing Center (TR-Grid e-Infrastructure). The authors are indebted to The Scientific and Technological Research Council of Turkey (Grant TUBITAK-114Z634) for financial support of this work.

Supplementary materials

Supplementary material associated with this article can be found, in the online version, at doi:10.1016/j.molstruc.2022.133414.

References

[1] J. Ferlay, M. Ervik, F. Lam, M. Colombet, L. Mery, M. Piñeros, et al., in: Global Cancer Observatory: Cancer today. Lyon, International Agency for Research on Cancer, 2018, p. 2020.
[2] https://www.who.int/news-room/fact-sheets/detail/cancer. Cancer 2021 [cited 2021 16. November].
[3] Y. Tang, Y. Wang, M.F. Kiani, B. Wang, Classification, treatment strategy, and associated drug resistance in breast cancer, Clin. Breast Cancer 16 (5) (2016) 335–343.
[4] S. Matou-Nasri, H. Sharaf, Q. Wang, N. Almobadel, Z. Rabhan, H. Al-Eidi, et al., Biological impact of advanced glycation endproducts on estrogen receptor-positive MCF-7 breast cancer cells, Biochim. Biophys. Acta (BBA) Mol. Basis Dis. 1863 (11) (2017) 2808–2820.
[5] C.H. Yip, A. Rhodes, Estrogen and progesterone receptors in breast cancer, Fut. Oncol. 10 (14) (2014) 2293–2301.
[6] Chapter three - N. Fuentes, P. Silveyra, Estrogen receptor signaling mechanisms, in: R. Donev (Ed.), Advances in Protein Chemistry and Structural Biology, 116, Academic Press, 2019, pp. 135–170.
[7] N. Kumar, H.K. Gulati, A. Sharma, S. Heer, A.K. Jassal, L. Arora, et al., Most recent strategies targeting estrogen receptor alpha for the treatment of breast cancer, Mol. Divers. 25 (1) (2021) 603–624.
[8] H.K. Patel, T. Bihani, Selective estrogen receptor modulators (SERMs) and selective estrogen receptor degraders (SERDs) in cancer treatment, Pharmacol. Ther. 186 (2018) 1–24.
[9] W. Yue, R.J. Santen, J.P. Wang, Y. Li, M.F. Verderame, W.P. Bocchinfuso, et al., Genotoxic metabolites of estradiol in breast: potential mechanism of estradiol-induced carcinogenesis, J. Steroid Biochem. Mol. Biol. 86 (3) (2003) 477–486.
[10] M.J. Duffy, Estrogen receptors: role in breast cancer, Crit. Rev. Clin. Lab. Sci. 43 (4) (2006) 325–347.
[11] F. Janku, D.J. McConkey, D.S. Hong, R. Kurzrock, Autophagy as a target for anti-cancer therapy, Nat. Rev. Clin. Oncol. 8 (9) (2011) 528–539.
[12] S.C. Lai, R.J. Devenish, LC3-associated phagocytosis (LAP): connections with host autophagy, Cells 1 (3) (2012) 396–408.
[13] D.J. Klionsky, S.D. Emr, Autophagy as a regulated pathway of cellular degradation, Science 290 (5497) (2000) 1717–1721.
[14] Y. Li, L. Wang, L. Pappan, A. Galliher-Beckley, J. Shi, IL-1β promotes stemness and invasiveness of colon cancer cells through Zeb1 activation, Mol. Cancer 11 (1) (2012) 1–13.
[15] H. Gezegen, C. Hepokur, U. Tutar, M. Ceylan, Synthesis and biological evaluation of novel 1-(4-(hydroxy(1-oxo-1,3-dihydro-2H-inden-2-ylidene)methyl) phenyl)-3-phenylurea derivatives, Chem. Biodivers. 14 (10) (2017) e1700223.
[16] R. Dennington, T. Keith, J.M. Millam, GaussView, Version 6.1, Semichem Inc., Shawnee Mission, KS, 2016.
[17] M.J. Frisch, G.W. Trucks, H.B. Schlegel, G.E. Scuseria, M.A. Robb, J.R. Cheeseman, G. Scalmani, V. Barone, G.A. Petersson, H. Nakatsuji, X. Li, M. Caricato, A.V. Marenich, J. Bloino, B.G. Janesko, R. Gomperts, B. Mennucci, H.P. Hratchian, J.V. Ortiz, A.F. Izmaylov, J.L. Sonnenberg, D. Williams-Young, F. Ding, F. Lipparini, F. Egidi, J. Goings, B. Peng, A. Petrone, T. Henderson, D. Ranasinghe, V.G. Zakrzewski, J. Gao, N. Rega, G. Zheng, W. Liang, M. Hada, M. Ehara, K. Toyota, R. Fukuda, J. Hasegawa, M. Ishida, T. Nakajima, Y. Honda, O. Kitao, H. Nakai, T. Vreven, K. Throssell, J.A. Montgomery, J.E. Peralta, F. Ogliaro, M.J. Bearpark, J.J. Heyd, E.N. Brothers, K.N. Kudin, V.N. Staroverov, T.A. Keith, R. Kobayashi, J. Normand, K. Raghavachari, A.P. Rendell, J.C. Burant, S.S. Iyengar, J. Tomasi, M. Cossi, J.M. Millam, M. Klene, C. Adamo, R. Cammi, J.W. Ochterski, R.L. Martin, K. Morokuma, O. Farkas, J.B. Foresman, D.J. Fox, Gaussian 16, Revision B.01, Gaussian, Inc., Wallingford CT, 2016.
[18] PerkinElmer, ChemBioDraw Ultra Version (13.0.0.3015), 2012.
[19] R.A. Friesner, R.B. Murphy, M.P. Repasky, L.L. Frye, J.R. Greenwood, T.A. Halgren, P.C. Sanschagrin, D.T. Mainz, Extra precision glide: docking and scoring incorporating a model of hydrophobic enclosure for protein-ligand complexes, J. Med. Chem. 49 (2006) 6177–6196.
[20] Schrödinger Release 2021-2: Epik, Schrödinger, LLC, New York, NY, 2021.
[21] Schrödinger Release 2021-2: Protein Preparation Wizard, Prime, Schrödinger, LLC, New York, NYNew York, NY, 2021 Epik, Schrödinger, LLC, New York, NY, 2021; Impact, Schrödinger, LLC.
[22] Schrödinger Release 2021-2: SiteMap, Schrödinger, LLC, New York, NY, 2021.
[23] H. Ataseven, K. Sayin, B. Tüzün, M.A. Gedikli, Could boron compounds be effective against SARS-CoV-2? Bratisl. Lek. Listy 122 (10) (2021) 753–758 01 Jan.
[24] M.A. Gedikli, B. Tuzun, K. Sayin, H. Ataseven, Determination of inhibitor activity of drugs against the COVID-19, Bratisl. Lek. Listy 122 (7) (2021) 497–506 01 Jan.
[25] M.A. Gedikli, B. Tuzun, A. Aktas, K. Sayin, H. Ataseven, Are clarithromycin, azithromycin and their analogues effective in the treatment of COVID19, Bratısl. Med. J. Bratısl. Lek. Lısty (2021) cilt.122, sa.2, ss.101-110.
[26] B. Tuzun, T. Nasibova, E. Garaev, K. Sayin, H. Ataseven, Could Peganum harmala be effective in the treatment of COVID-19? Bratisl. Lek. Listy 122 (9) (2021) 670–679 01 Jan.
[27] E. Center, K. Sayin, B. Tuzun, H. Ataseven, Could boron-containing compounds (BCCs) be effective against SARS-CoV-2 as anti-viral agent? Bratisl. Lek. Listy 122 (4) (2021) 263–269 01 Jan.
[28] M. Ergül, K. Sayin, H. Ataseven, 2-phenylethyne-1-sulfonamide derivatives as new drugs candidates for heat shock protein 70 and doublecortin-like kinase, Turkish Comput. Theor. Chem. 5 (1) (2021) 1–12.
[29] J.M.M. Levy, C.G. Towers, A. Thorburn, Targeting autophagy in cancer, Nat. Rev. Cancer 17 (9) (2017) 528–542.
[30] M.I. Koukourakis, D. Kalamida, A. Giatromanolaki, C.E. Zois, E. Sivridis, S. Pouliliou, et al., Autophagosome proteins LC3A, LC3B and LC3C have distinct subcellular distribution kinetics and expression in cancer cell lines, PLoS One 10 (9) (2015) e0137675.
[31] H.Y. Zheng, X.Y. Zhang, X.F. Wang, B.C. Sun, Autophagy enhances the aggressiveness of human colorectal cancer cells and their ability to adapt to apoptotic stimulus, Cancer Biol. Med. 9 (2) (2012) 105–110 Epub 2013/05/22.
[32] S. Bortnik, B. Tessier-Cloutier, S. Leung, J. Xu, K. Asleh, S. Burugu, et al., Differential expression and prognostic relevance of autophagy-related markers ATG4B, GABARAP, and LC3B in breast cancer, Breast Cancer Res. Treat. 183 (3) (2020) 525–547.
[33] H. Zhao, M. Yang, J. Zhao, J. Wang, Y. Zhang, Q. Zhang, High expression of LC3B is associated with progression and poor outcome in triple-negative breast cancer, Med. Oncol. 30 (1) (2013) 475.
[34] C.H. Lee, J.S.M. Chang, S.H. Syu, T.S. Wong, J.Y.W. Chan, Y.C. Tang, et al., IL-1β promotes malignant transformation and tumor aggressiveness in oral cancer, J. Cell. Physiol. 230 (4) (2015) 875–884.
[35] C. Rébé, F. Ghiringhelli, Interleukin-1β and Cancer, Cancers 12 (7) (2020) 1791.
[36] G. Cui, A. Yuan, Z. Sun, W. Zheng, Z. Pang, IL-1β/IL-6 network in the tumor microenvironment of human colorectal cancer, Pathol. Res. Pract. 214 (7) (2018) 986–992.
[37] K. Tawara, H. Scott, J. Emathinger, C. Wolf, D. LaJoie, D. Hedeen, et al., HIGH expression of OSM and IL-6 are associated with decreased breast cancer survival: synergistic induction of IL-6 secretion by OSM and IL-1β, Oncotarget 10 (21) (2019) 2068–2085 Epub 2019/04/23.